

ZEKE and Hole-Burning Spectroscopy of the Rotational Isomers of Resorcinol·CO

Wolf D. Geppert, Caroline E. H. Dessent, and Klaus Müller-Dethlefs*

Department of Chemistry, University of York, Heslington, York, YO10 5DD, U.K.

Received: July 23, 1999; In Final Form: September 24, 1999

Two rotational isomers of resorcinol·CO were investigated using zero electron kinetic energy (ZEKE) photoelectron spectroscopy. Vibrational progressions and combination bands of the in-plane-bend, stretch and in-plane-wag intermolecular modes were observed in the spectra of each isomer. While the frequencies of these intermolecular modes were similar for both isomers, the Franck–Condon patterns for vibrational excitation were notably different, indicating that the isomers experience distinctive geometry changes upon ionization. Ab initio calculations at the MP2/6-31G* level of theory predict the existence of many stable isomers of resorcinol·CO, with the three lowest energy minima corresponding to structures where the CO molecule binds through its carbon atom to one OH group of resorcinol. The calculations were used to assign the vibrational features in the ZEKE spectra and distinguish the rotational isomers observed.

I. Introduction

Intermolecular bonds play an important role in many areas of chemistry and biology from ion solvation to macromolecular structure.¹ A detailed knowledge of the intermolecular potential energy surface is essential if these interactions are to be understood from a microscopic perspective. The interactions in closed shell systems in their ground electronic states have been well characterized from an experimental and theoretical viewpoint,² and it has recently been possible to construct potential surfaces with spectroscopic accuracy for Ar₂·DCl and Ar·HF.^{3,4} This situation is quite different for ionic complexes, which have proven more spectroscopically challenging, and it is only over the past decade that a number of methods have emerged which allow the characterization of both cationic and anionic complexes.^{5–13}

Zero electron kinetic energy (ZEKE) photoelectron spectroscopy has developed into one of the most powerful, high-resolution photoelectron spectroscopic techniques for studying cationic molecular complexes.^{5–11} Since the resolution of the method is often not sufficient to obtain rotational resolution for moderately large systems, the general approach for elucidating the structure of a complex using ZEKE spectroscopy relies on the comparison of intermolecular vibrational frequencies obtained from the ZEKE spectrum with harmonic frequencies from an ab initio calculation. This procedure has been demonstrated to be reliable in a number of cases where additional experimental results have corroborated geometric structures obtained from this approach. A recent example is provided by the ZEKE spectrum of [phenol·N₂]⁺,¹⁴ where ab initio calculations pointed to a hydrogen-bonded in-plane structure,¹⁵ which was subsequently supported by direct evidence from an infrared spectrum of the cation.¹⁶

We have recently studied three rotational isomers of the resorcinol (1,3-dihydroxybenzene)·H₂O complex using resonance enhanced multiphoton ionization (REMPI) and ZEKE spectroscopies, along with ab initio calculations.¹⁷ The barrier for rotation of an OH group in resorcinol is substantial (~1200 cm⁻¹),^{18,19} facilitating the isolation of different isomers in a molecular beam expansion. Since the intermolecular geometries are broadly similar for a series of rotational isomers, the

vibrational spectra of the complexes provide a useful benchmark for ab initio calculations, which should predict subtle differences in the isomeric intermolecular bonds. In resorcinol·H₂O, the calculations reproduced the experimental frequencies of the intermolecular vibrations reasonably well, although some discrepancies did appear between the predicted geometry changes and the Franck–Condon (FC) patterns of vibrational progressions.

In this paper, we present a study of resorcinol·CO, where REMPI and ZEKE spectroscopy are used to explore different solvent binding sites which are available in rotational isomers. Although the quadrupolar CO molecule forms a hydrogen-bonding type interaction with aromatic OH groups,^{15,20} the interaction is considerably weaker than for the water ligand. We anticipate that the primary interaction in resorcinol·CO should involve this type of weak hydrogen bond where the CO binds to the OH group of phenol through its carbon atom. To assess the extent to which the primary intermolecular bond of resorcinol·CO is perturbed by the second OH group of resorcinol, we compare the resorcinol·CO ZEKE spectra with the spectra of phenol·CO and use ab initio calculations to aid the interpretation of the spectra.

II. Experimental Section

The technique and apparatus used for the experiments have been described in detail previously.^{9,14} Resorcinol·CO clusters were prepared by expanding the heated (370–420 K) resorcinol sample seeded in a 5% CO/neon mixture at 0.5–1.5 bar through a 200 μm nozzle (General Valve Series 9) while pure neon was used for recording the monomer spectrum. The skimmed supersonic beam was intersected by the beams of two frequency-doubled dye lasers (Radiant Narrowscan to perform the initial excitation to an S₁ intermediate state and Lambda Physik FL 3002 to effect ionization) pumped synchronously by an excimer laser (Lambda Physik EMG 1003i). Hole-burning experiments²¹ were carried out using the procedure described in ref 17.

Spectra were normalized to dye laser intensity and calibrated by simultaneously recording iodine spectra²² with all quoted laser photon energies having been converted from air to vacuum. Ionization energies (IE) have been corrected for field effects

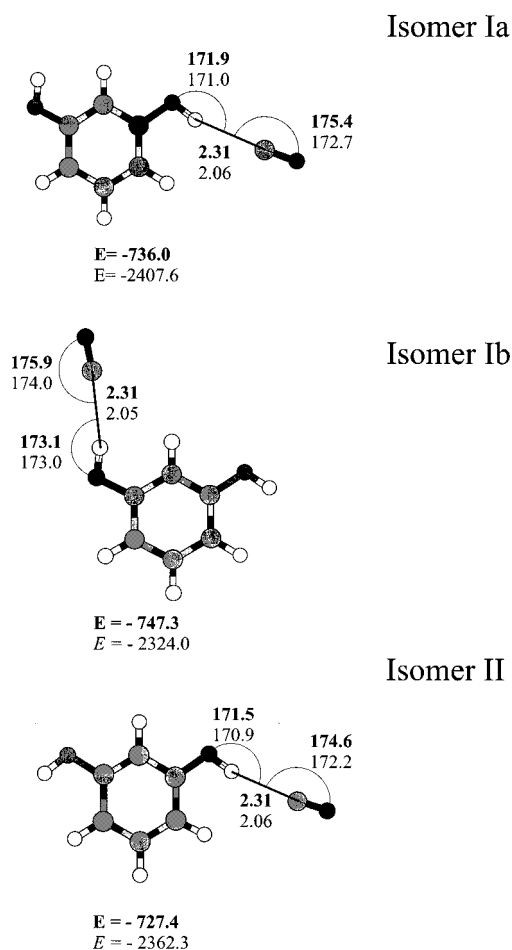


Figure 1. Geometrical structures and counterpoise corrected binding energies of three rotational isomers of resorcinol·CO obtained at the MP2/6-31G* level of theory. Bold figures refer to the neutral ground state, while figures in plain text refer to the ionic ground state. Energies are given in cm^{-1} , bond lengths in Å, and angles in degrees.

by extrapolation to zero field using the formula $\Delta E = 4F^{1/2}$ where ΔE is the field shift in cm^{-1} and F is the field strength in V/cm .²³ Errors reported for the peak positions reflect the laser calibration accuracy ($\pm 0.02 \text{ cm}^{-1}$) and the full-widths-at-half-maximum.

III. Ab Initio Calculations of Resorcinol·CO

The structures of the neutral (S_0) and cationic (D_0) ground states of resorcinol·CO were obtained from ab initio calculations at the restricted and unrestricted MP2/6-31G* levels of theory using *Gaussian 94* (the OPT=TIGHT option was used for all optimizations).^{24,25} This level of theory had reproduced the experimental intermolecular mode frequencies reasonably well in the related phenol·CO cluster.¹⁵ In a previous REMPI study, Gerhards et al.²⁶ observed only two rotational isomers of the resorcinol monomer (see Figure 2 for schematics of these structures), and therefore only structures where the CO moiety binds to these isomers were pursued in this study. Harmonic frequencies were computed to confirm that optimized structures correspond to local minima.

Geometry optimizations were conducted on a large number of structures, with the three lowest energy isomers identified being presented in Figure 1. Corresponding minima exist for each isomer with the oxygen atom of CO binding to the phenolic OH group. However, as in phenol·CO,¹⁵ the “oxygen in” isomers correspond to substantially higher energy structures and are not

TABLE 1: Ab Initio Harmonic Frequencies (cm^{-1}) of the Intermolecular Vibrations of the Rotational Isomers of [Resorcinol·CO]⁺ at the UMP2/6-31G* Level of Theory^a

mode	ab initio frequencies			experimental frequencies			
	isomer Ia	isomer Ib	isomer II	isomer I		isomer II	
	ω_e	$\omega_e x_e$	ω_e	ω_e	$\omega_e x_e$	ω_e	$\omega_e x_e$
β''	32.0	38.4	31.4				
β'	44.1	38.4	43.5	33.3	0.1	37.0 ^b	-
σ	127.9	132.6	126.8	125.0	2.4	120.0	2.2
γ''	152.7	158.2	150.8				
γ'	164.3	163.3	162.2	151.0	2.0	156.0 ^b	

^a Experimental ω_e and $\omega_e x_e$ values are also presented for comparison with the ab initio results. ^b Frequency from the IE feature since only $\nu = 1$ features were observed for these modes.

considered further.²⁷ The intermolecular binding energies (counterpoise corrected) and geometric parameters for the S_0 and D_0 states of the isomers are included in Figure 1. The intermolecular vibrational frequencies of the cations are listed in Table 1.

The structure of each of the resorcinol·CO isomers resembles that of phenol·CO,¹⁵ possessing C_s symmetry and CO “carbon in” binding. In the neutral structures, the intermolecular bond angles are quite similar to those obtained for phenol·CO, with the isomer Ib parameters deviating most from the phenol·CO values. For example, the $\text{H}\cdots\text{C}-\text{O}$ angle is 175.4, 175.9, and 174.6° for isomers Ia, Ib, and II, respectively, versus 174.5° for phenol·CO. The same pattern is repeated in the cationic complexes, although for isomers Ia and II the angles are now slightly smaller than in phenol·CO whereas the isomer Ib angle is slightly larger (172.7, 174.0, and 172.2° for isomers Ia, Ib, and II versus 173.7° for phenol·CO). The intermolecular bond length is marginally smaller in each neutral complex, but larger in the cationic isomers compared to the phenol cluster ($r = 2.317 \text{ Å}$ for phenol·CO and 2.040 Å for [phenol·CO]⁺). Comparing the counterpoise corrected interaction energies calculated for phenol·CO in ref 15 with the values for resorcinol·CO (Figure 1), it is notable that while the S_0 state is more strongly bound in resorcinol·CO, [phenol·CO]⁺ is more strongly bound in the D_0 state.

IV. Experimental Results and Discussion

A. The REMPI Spectrum of Resorcinol·CO. The (1+1') two-color REMPI spectrum of the resorcinol monomer is presented in Figure 2a for comparison with the REMPI spectrum of resorcinol·CO. Gerhards et al.²⁶ have assigned the prominent features at 35944 and 36196 cm^{-1} to the S_10^0 transitions of isomers I and II, depicted in Figure 2a. The (1+1') two-color REMPI spectrum of resorcinol·CO is presented in Figure 2b. Fragmentation and dissociation of higher clusters into lower mass channels were minimized by setting the ionization laser to 30800 cm^{-1} for both REMPI spectra. The REMPI spectrum of resorcinol·CO is dominated by two strong features at 35808 ± 1 and 36100 $\pm 1 \text{ cm}^{-1}$, which are assigned to the S_10^0 transitions of two isomers of resorcinol·CO. To rule out the presence of other resorcinol·CO isomers which might have higher ionization thresholds, an additional REMPI spectrum was recorded with the ionization laser set to higher energy (31500 cm^{-1}). No evidence for prominent additional isomers was observed in that spectrum or in the (1+1) one-color REMPI spectrum presented in Figure 3a.

The S_10^0 features can be related to the monomer rotational isomers by considering the spectral shifts of the cluster S_10^0 transitions relative to the respective monomer transitions. In phenol·CO, the S_10^0 transition is red shifted by 190 cm^{-1}

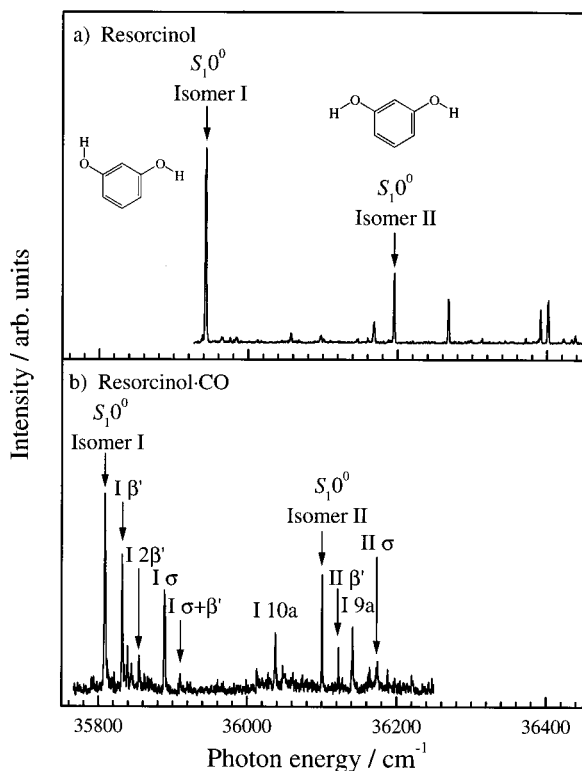


Figure 2. $(1+1')$ two-color REMPI spectra of (a) resorcinol and (b) resorcinol·CO with the ionizing laser set to 30800 cm^{-1} . Schematic structures of resorcinol isomers I and II are included on Figure 2a. Assignments of the in-plane bend (β') and stretch (σ) are included on Figure 2b.

compared to the corresponding transition in phenol,²⁰ and we anticipate that similar red shifts should be observed for the resorcinol·CO isomers. The feature at $35808 \pm 1\text{ cm}^{-1}$ can therefore be associated with CO complexing to resorcinol isomer I with a red shift of 136 cm^{-1} , while the feature at $36100 \pm 1\text{ cm}^{-1}$ can be associated with CO complexing to isomer II with a red shift of 96 cm^{-1} . The $S_1 0^0$ transition red shifts of the two resorcinol·CO isomers are smaller than the phenol·CO value, in line with our recent resorcinol·H₂O study,¹⁷ where smaller $S_1 0^0$ red shifts (320 , 249 , and 291 cm^{-1}) were observed compared to phenol·H₂O (352.5 cm^{-1}).

A number of less intense peaks are also visible in the resorcinol·CO REMPI spectrum, which were assigned by comparison with the REMPI spectra of phenol·CO²⁰ and resorcinol.²⁶ Spectral features are listed in Table 2 along with assignments. For both isomers it is notable that the intermolecular modes appear at lower frequencies than the analogous modes of phenol·CO.²⁰ This observation indicates that the CO molecule is bound more weakly in the S_1 state to resorcinol than phenol, in line with the comparatively smaller red shifts of the resorcinol·CO complexes. For both isomers, the relative intensities of the $S_1 0^0$, in-plane-bend, and stretch transitions are similar to those observed in the phenol·CO REMPI spectrum and indicate that similar geometry changes occur during $S_1 \leftarrow S_0$ excitation in both systems.

Hole-burning (HB) spectra²¹ were recorded to confirm that two isomers are present in the REMPI spectrum of resorcinol·CO. Figure 3a shows a one-color $(1+1)$ REMPI spectrum of the resorcinol·CO cluster for comparison with the HB spectra. Figure 3b presents the spectrum obtained with the HB laser set to the isomer I $S_1 0^0$ transition. The spectrum clearly indicates that two distinct species are present in the REMPI spectrum since the features associated with the $S_1 0^0$ transition of

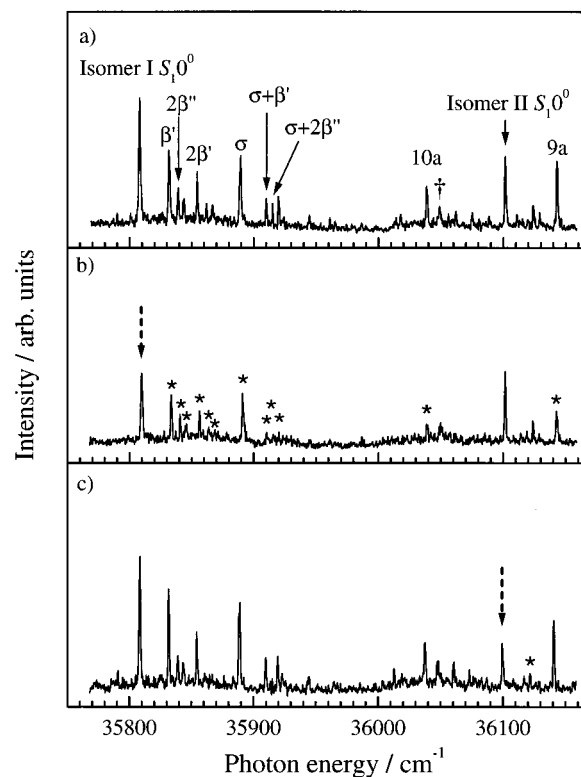


Figure 3. Hole-burning spectra of resorcinol·CO with (a) no hole-burning laser (one-color $(1+1)$ REMPI spectrum), (b) the hole-burning laser set to the $S_1 0^0$ transition of isomer I and (c) to the $S_1 0^0$ transition of isomer II. The hole-burning laser position is marked with dashed arrows, and bands affected are marked with asterisks. The band marked † is not associated with isomer I or II; see text for discussion.

TABLE 2: Frequencies of Vibrational Features Observed in the REMPI Spectrum of Resorcinol·CO^a

$S_1 \leftarrow S_0$ energy/ cm^{-1}	assignment	$S_1 \leftarrow S_0$ energy/ cm^{-1}	assignment
35808 _s	I $S_1 0^0$	36013 _w	? ^b
35832 _s	I β'	36038 _m	I 10a
35839 _m	I $2\beta''$	36048 _w	? ^b
35844 _w	I $\beta' + \beta''$	36100 _s	II $S_1 0^0$
35854 _m	I $2\beta'$	36123 _m	II β'
35889 _s	I σ	36142 _m	I 9a
35910 _w	I $\sigma + \beta'$	36164 _w	I 9a + β'
35915 _w	I $\sigma + 2\beta''$	36175 _w	II σ

^a Intensities are denoted as w (weak), m (medium), and s (strong).

^b The ? indicates a peak which could not be assigned.

resorcinol·CO isomer II are unaffected by the burn laser. This result is confirmed by the spectrum presented in Figure 3c where the burn laser was set to the isomer II $S_1 0^0$ transition, and the only feature affected by the burn laser was the $S_1 \beta'$ band of the same isomer. We note that the feature labeled † in Figure 3a does not appear to be associated with either isomer I or II and may, therefore, indicate the presence of the third isomer of resorcinol·CO (Figure 1). It was not possible to record a ZEKE spectrum via this transition due to the weak nature of the feature. However, while three resorcinol·CO isomers should exist, it seems very improbable that this feature represents the $S_1 0^0$ transition of the “missing” isomer Ia or Ib complex, since its origin transition would then be blue shifted by 106 cm^{-1} compared to the respective monomer transition. We note that this feature could arise from fragmentation of higher clusters into this mass channel.

B. ZEKE Spectra of Resorcinol·CO. (i) *Resorcinol·CO Isomer I.* ZEKE spectra recorded via three different S_1 states of resorcinol·CO isomer I are displayed in Figure 4. The lowest

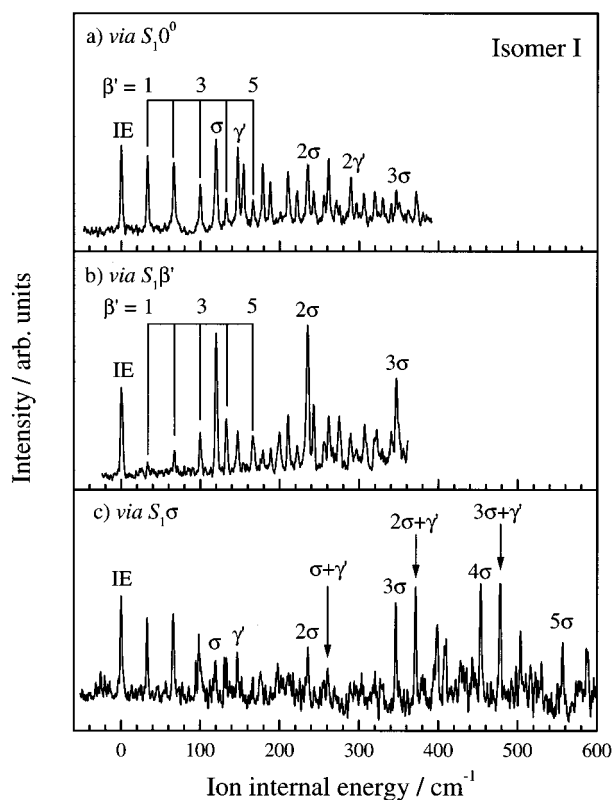


Figure 4. ZEKE spectra of resorcinol·CO isomer I via three different intermediate S_1 levels: (a) $S_{1,0^0}$, (b) $S_{1,\beta'}$, and (c) $S_{1,\sigma}$. Assignments of the in-plane wag (γ'), in-plane bend (β'), and stretch (σ) are included on the spectra.

TABLE 3: Frequencies (cm^{-1}) of Vibrational Features Observed in the ZEKE Spectra of Isomer I of [Resorcinol·CO] $^+$ via Three Different Intermediate S_1 States a

$S_{1,0^0}$	$S_{1,\beta'}$	$S_{1,\sigma}$	assignment	$S_{1,0^0}$	$S_{1,\beta'}$	$S_{1,\sigma}$	assignment
33s	33w	33s	β'	276m	275s		$\gamma'+4\beta'$
67s	67m	66s	$2\beta'$	290s	289m		$2\gamma'$
100s	100m	99s	$3\beta'$	297m	297w		$\sigma+\gamma'+\beta'$
120s	120s	120m	σ	306m	307m		$\gamma'+5\beta'$
133m	133s	133m	$4\beta'$	320m	322m		$2\gamma'+\beta'$
147s	147m	147m	γ'	329m			$\sigma+\gamma'+2\beta'$
155s			$\sigma+\beta'$	340m	341m		$\gamma'+6\beta'$
167m	166m	166w	$5\beta'$	347m	347s	347s	3σ
179s	179m	177w	$\gamma'+\beta'$	350m			$2\gamma'+2\beta'$
188s	189m		$\sigma+2\beta'$	372m		372s	$2\sigma+\gamma'$
201w	200m	199w	$6\beta'$			380w	$3\sigma+\beta'$
210s	211s		$\gamma'+2\beta'$			399s	$\sigma+2\gamma'$
222m	222m		$\sigma+3\beta'$			410s	16b
236s	235s	236m	2σ			453s	4σ
243m	243s		$\gamma'+3\beta'$			479s	$3\sigma+\gamma'$
256m	256m		$\sigma+4\beta'$			504s	$2\sigma+2\gamma'$
262s	262s	261w	$\sigma+\gamma'$			556s	5σ
272m			$2\sigma+\beta'$			587m	$5\sigma+\beta'$

a Frequencies are given relative to the IE and intensities are denoted as w (weak), m (medium), and s (strong).

energy feature in all three spectra is assigned to the vibrational ground state of the cation, which corresponds to an IE (computed as the sum of the $S_{1,0^0}$ transition and the field corrected vibrationless $D_0 \leftarrow S_1$ transition) of $65293 \pm 3 \text{ cm}^{-1}$. This amounts to a red shift of $1402 \pm 7 \text{ cm}^{-1}$ relative to the monomer transition, 28 which is considerably smaller than the IE red shift of 1766 cm^{-1} observed in phenol·CO. 20 Vibrational features present in these spectra are listed in Table 3 and consist of features spaced by 33, 120, and 147 cm^{-1} . These features can be assigned by comparison with the ZEKE spectrum of phenol·CO as the in-plane bend (β'), stretch (σ), and in-plane wag (γ'),

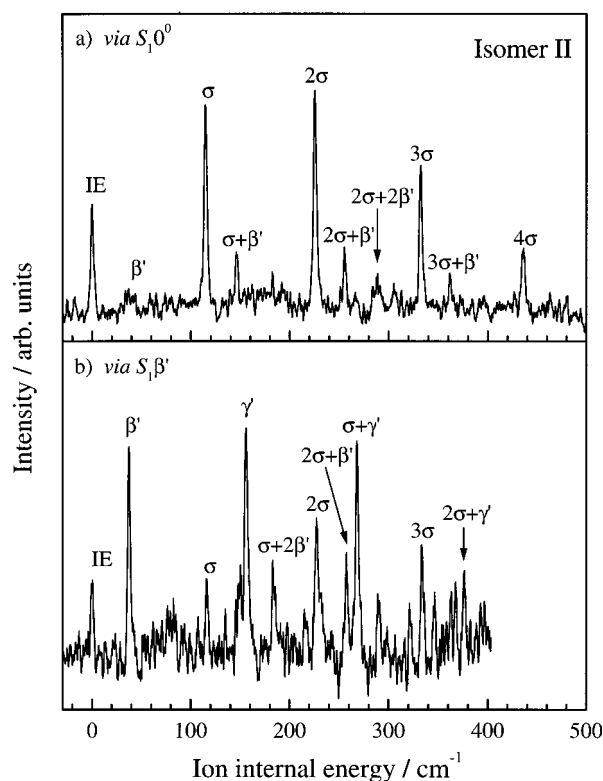


Figure 5. ZEKE spectra of resorcinol·CO isomer II via two different intermediate S_1 levels: (a) $S_{1,0^0}$ and (b) $S_{1,\beta'}$. Assignments of the in-plane wag (γ'), in-plane bend (β'), and stretch (σ) modes are included on the spectra.

respectively. 20 The frequencies of the observed intermolecular vibrations of isomer I of [resorcinol·CO] $^+$ are smaller than those of [phenol·CO] $^+$ (42, 130, and 160 cm^{-1}) indicating that a weaker interaction exists in the former cluster. This observation is in line with the ab initio calculations which predict stronger binding energies for [phenol·CO] $^+$. 15 Values of ω_e and $\omega_e x_e$ for these intermolecular modes are presented in Table 1.

The ZEKE spectrum recorded via the $S_{1,0^0}$ transition of isomer I (Figure 4a) is dominated by progressions in the β' and σ modes. While excitation of σ is a feature of the phenol·CO ZEKE spectrum, 20 the substantial excitation ($> \nu = 6$) of β' is distinctive. In phenol·CO only two quanta of β' were observable in the ZEKE spectrum recorded via the $S_{1,0^0}$ state, 20 indicating that the geometry change occurring along the β' coordinate upon $D_0 \leftarrow S_1$ excitation in isomer I is much larger than in phenol·CO. Since the FC factors of the intermolecular vibrations in the REMPI spectrum reveal that only a small geometry change occurs (section IV.A) upon $S_1 \leftarrow S_0$ excitation, the intermolecular geometry of resorcinol·CO isomer I must be markedly different from that of phenol·CO in the neutral and/or ionic complexes.

A ZEKE spectrum recorded via $S_{1,\beta'}$ is presented in Figure 4b and shows a progression in β' with a FC pattern which is significantly different from the spectrum via the S_1 origin, confirming the assignment of the mode in the REMPI spectrum. Figure 4c shows the ZEKE spectrum recorded via $S_{1,\sigma}$. The FC pattern of the σ mode is again substantially different from the spectrum recorded via $S_{1,0^0}$. Combination bands of σ with one quantum of γ' are also enhanced in this spectrum.

(ii) *Resorcinol·CO Isomer II.* ZEKE spectra of resorcinol·CO isomer II recorded via $S_{1,0^0}$ and $S_{1,\beta'}$ are shown in Figure 5, with the lowest energy feature in both spectra being assigned to the adiabatic IE as $65702 \pm 3 \text{ cm}^{-1}$. The distinct IEs of isomers I and II confirm the hole-burning results and demon-

TABLE 4: Frequencies (cm^{-1}) of Vibrational Features Observed in the ZEKE Spectra of Isomer II of [Resorcinol•CO]⁺ via Two Different S₁ Intermediate States^a

S ₁ 0 ⁰	S ₁ β'	assignment	S ₁ 0 ⁰	S ₁ β'	assignment
37w	37s	β'		268s	σ+γ'
116s	116m	σ	289w	289m	2σ+2β'
146m	150m	σ+β'		321m	2σ+3β'
	156s	γ'	332s	333m	3σ
	183m	F+2β'		347m	9a
215w		σ+3β'	361w		3σ+β'
226s	228s	2σ		376m	2σ+γ'
255m	258m	2σ+β'	436m		4σ

^a Frequencies are given relative to the IE and intensities are denoted by w (weak), m (medium), and s (strong).

strate that two isomeric species are present in the REMPI spectrum. The IE corresponds to a red shift of $1446 \pm 7 \text{ cm}^{-1}$ compared to the monomer IE.²⁸ Vibrational features present in the spectra are listed in Table 4 and consist of peaks separated by 37, 116, and 156 cm^{-1} , which are assigned by comparison with the phenol•CO ZEKE spectrum as β', σ, and γ', respectively.²⁰ The smaller frequencies of the intermolecular modes compared to phenol•CO again indicate that the CO interacts more weakly with resorcinol⁺ than phenol⁺. ω_e and ω_ex_e values for σ are presented in Table 1, for comparison with the isomer I values.

The ZEKE spectrum recorded via S₁0⁰ is presented in Figure 5a and reveals modest excitation of β', with the single quantum feature being only just visible above the baseline. *This FC pattern is remarkably different from the isomer I spectrum and indicates that a much smaller geometry change occurs along this coordinate upon ionization.* We note that the geometry change is also smaller than in phenol•CO.²⁰ Excitation of σ is, however, somewhat more pronounced than in the corresponding isomer I spectrum with the FC envelope of the σ progression resembling the one observed in the phenol•CO ZEKE spectrum recorded via S₁0⁰.

Figure 5b shows the ZEKE spectrum recorded via S₁β'. Since this transition is relatively weak in the REMPI spectrum, the signal-to-noise ratio is smaller than in the other ZEKE spectra presented. β' is strongly enhanced compared to the spectrum recorded via S₁0⁰, with the FC pattern strictly following the Δν = 0 propensity rule.⁵ Finally, we note that γ' and its combinations with σ are strongly enhanced in this spectrum compared to the spectrum recorded via S₁0⁰.

C. Comparison of the ZEKE Spectra and Ab Initio Results. In general, the ab initio and experimental results appear to be in broad agreement. The calculations predict that the resorcinol•CO isomers should adopt structures with intermolecular bonds resembling that of phenol•CO.¹⁵ ZEKE spectra of both resorcinol•CO isomers display excitation of three intermolecular vibrations, β', σ, and γ', as in phenol•CO,²⁰ with frequencies of similar magnitude. This leads to the conclusion that the resorcinol•CO structures can be characterized as having the CO ligand hydrogen bonded to a phenolic OH group within the aromatic plane. In phenol•CO, the ab initio harmonic frequencies were observed to be 10–15% larger than the experimental values using the same level of theory employed in this work.¹⁵ If we consider isomer II of resorcinol•CO, the β', σ, and γ' are spaced by 37, 116, and 156 cm^{-1} , respectively with the ab initio calculations predicting values of 44, 127, and 162 cm^{-1} . Therefore, as in phenol•CO,¹⁵ the theoretical predictions are less than 15% higher than the experimental results. (Table 1 illustrates that the anharmonicities of β', σ, and γ' for the resorcinol•CO isomers are similar to those observed for phenol•CO.²⁰) Finally, the ab initio calculations recover the

comparatively weaker binding of the [resorcinol•CO]⁺ complexes compared to [phenol•CO]⁺ evidenced in the lower frequencies of intermolecular vibrations in the ZEKE spectra.

In section IV.B, it was noted that the FC patterns of vibrational progressions in several intermolecular modes differed from those observed in phenol•CO. This was particularly noticeable for β', where resorcinol•CO isomer I displayed a much more extensive progression in this mode than phenol•CO, whereas isomer II displayed almost no excitation along this coordinate. To quantify this effect, FC simulations were conducted to analyze the geometry change along the β' coordinate using the method of Bieske et al.²⁹ A harmonic oscillator potential was used,³⁰ with $\mu_{\text{bx}}^{1/2} \tan \Delta \varphi$ as a coordinate (μ_{bx} represents the reduced mass for distortion²⁹ and Δφ the change in the H•••C–O angle between the S₁ and D₀ states). Here, μ_{bx} was calculated from structural parameters taken from the ab initio calculations, while the force constant $k = \mu_{\text{bx}}(2\pi c\nu)^2$ for the harmonic oscillator potential was calculated using experimental values of ν (for β') in the relevant states. These simulations replicated the β' FC pattern with changes of 9.9, 9.6, and 3.4° for the H•••C–O angle of isomers Ia, Ib and II, whereas the calculations predict changes of 2.7, 1.9 and 2.4°, respectively.

A second set of FC simulations were performed to quantify changes along the σ coordinate upon ionization for both isomers using a simple one-dimensional potential. The FC patterns were accurately replicated with reductions of the intermolecular bond from S₁ to D₀ by 0.20 Å for isomer I and 0.27 Å for isomer II. The ab initio calculations predict changes of 0.25, 0.26, and 0.25 Å for isomers Ia, Ib, and II from the S₀ to the D₀ states. Since little structural change occurs for S₁←S₀ excitation (see section IV.A), both simulations point to the structural changes that occur upon ionization of isomer I not being accurately reproduced by the calculations. This discrepancy can probably be attributed to the theoretical level of the ab initio calculations, which is most likely to affect the more weakly bound S₀ state. CO possesses a small dipole moment which is notoriously difficult to calculate using HF or MP2 ab initio theory and has led to problems in computational studies of the H₂O•CO complex.^{31,32} If the electrostatic charges on CO are not properly replicated, the structure of isomer Ib is most likely to be affected since, in this isomer, the oxygen of the CO ligand can also interact with the distant oxygen of the second OH group of resorcinol. (We note that it is also possible that the one-dimensional FC simulations employed may not be sufficient, e.g. if a coupling exists between intermolecular vibrations, or a Dushinsky rotation accompanies ionization.)

D. Assignment of the Rotational Isomers of Resorcinol•CO. Unlike resorcinol•H₂O,¹⁷ we found no evidence for the presence of the third rotational isomer of resorcinol•CO in this study. It is currently unclear why only two of the isomers are formed under the free jet expansion conditions employed, although this phenomenon presumably relates to different barrier heights for interconversion of isomers Ia and Ib in the two systems. The barrier heights for motion of the relatively weakly interacting CO molecule should certainly be lower than for water. While further ab initio calculations could provide barrier heights for these systems, calculations of the potential energy surface of resorcinol•CO were considered beyond the scope of this work.

On the basis of the calculated binding energies (Figure 1), the formation of isomer Ib should be favored over isomer Ia. If we take the results for isomer II as a benchmark, this assignment is reinforced by a comparison of the experimental and calculated

intermolecular frequencies of isomer I. The calculations (Table 1) predict that the frequencies of β' and σ are similar for isomers Ia and II with the isomer Ib β' frequency being somewhat lower, while the Ib σ frequency is higher, as observed in the ZEKE data. This conclusion is also in line with our resorcinol·H₂O results, where the ZEKE spectra of the corresponding resorcinol·H₂O isomers Ia and II were built on progressions of intermolecular modes with very similar frequencies, while the isomer Ib complex displayed distinctive vibrational frequencies. While the intermolecular bond in isomers Ia and II should closely resemble the bond in the respective phenol cluster, the isomer Ib structure may benefit from an additional electrostatic interaction between the ligand and the oxygen of the second OH group of resorcinol. Although this interaction would stabilize the neutral ground state,¹⁷ it is repulsive in the cation and could produce the substantial β' geometry change upon D₀←S₀ excitation observed in the ZEKE spectra of resorcinol·CO isomer I. However, given that some discrepancy exists between the ab initio calculations and experimental data (see section IV.C), the assignment of the isomer I structure as isomer Ib must be viewed as tentative until either higher level calculations or additional experimental data (e.g., spectra of deuterated resorcinol or MATI dissociation energies) are obtained.

Acknowledgment. We thank the Engineering and Physical Science Research Council (Grant No. Chemistry GR/L27770) for financial support of this work.

References and Notes

- Hobza, P.; Zahradnik, R. *Intermolecular complexes: The role of van der Waals systems in physical chemistry and in the biosciences*; Elsevier: Amsterdam, 1988.
- Bacic, Z.; Miller, R. E. *J. Phys. Chem.* **1996**, *100*, 12945.
- Elrod, M. J.; Saykally, R. J.; Cooper, A. R.; Hutson, J. M. *Mol. Phys.* **1994**, *81*, 579.
- Hutson, J. M. *J. Chem. Phys.* **1992**, *96*, 6752.
- Müller-Dethlefs, K.; Schlag, E. W. *Angew. Chem., Int. Ed. Engl.* **1998**, *37*, 1346.
- Cockett, M. C. R.; Müller-Dethlefs, K.; Wright, T. G. *Annu. Rep. Prog. Chem. Sect. C: Phys. Chem.* **1998**, *94*, 327.
- Müller-Dethlefs, K.; Cockett, M. C. R. In *Nonlinear Spectroscopy for Molecular Structure Determination*; Field, R. W., Ed.; Blackwell Science: Oxford, England, 1998; Chapter 7.
- Müller-Dethlefs, K.; Dopfer, O.; Wright, T. G. *Chem. Rev.* **1994**, *94*, 1845.
- Müller-Dethlefs, K.; Schlag, E. W.; Grant, E. R.; Wang, K.; McKoy, B. V. *Advanced Chemistry and Physics XC*; Wiley: Chichester, England, 1995.
- Müller-Dethlefs, K. In *High-Resolution Laser Photoionisation and Photoelectron Studies*; Powis, I., Baer, T., Ng, C. Y., Eds.; J. Wiley and Sons: Chichester, England, 1995; Chapter 2.
- (a) Lembach, G.; Brutschy, B. *J. Phys. Chem. A* **1998**, *102*, 6068. (b) Siglow, K.; Neuhauser, R.; Neusser, H. J. *J. Chem. Phys.* **1999**, *110*, 5589. (c) Pitts, J. D.; Knee, J. L.; Wategaonkar, S. *J. Chem. Phys.* **1999**, *110*, 3378. (d) Sato, S.; Omiya, K.; Kimura, K. *J. Electron. Spectrosc. Relat. Phenom.* **1998**, *97*, 121. (e) Hobza, P.; Spirko, V.; Selzle, H. L.; Schlag, E. W. *J. Phys. Chem. A* **1998**, *102*, 2501. (f) Held, A.; Selzle, H. L.; Schlag, E. W. *J. Phys. Chem. A* **1998**, *102*, 9625.
- (a) Dopfer, O.; Olkhov, R. V.; Maier, J. P. *J. Phys. Chem. A* **1999**, *103*, 2982. (b) Carrington, A. *Science* **1996**, *274*, 1327. (c) Duncan, M. A. *Annu. Rev. Phys. Chem.* **1997**, *48*, 69. (d) Lisy, J. M. In *Cluster ions*; Ng, C. Y., Baer, T., Powis, I., Eds.; Wiley: New York, 1993.
- (a) Bailey, C. G.; Kim, J.; Dessent, C. E. H.; Johnson, M. A. *Chem. Phys. Lett.* **1997**, *269*, 122. (b) Ayotte, P.; Weddle, G. H.; Kim, J.; Johnson, M. A. *Chem. Phys.* **1998**, *239*, 485. (c) Cabarcos, O. M.; Weinheimer, C. J.; Lisy, J. M.; Xantheas, S. S. *J. Chem. Phys.* **1999**, *110*, 5. (d) Choi, J. H.; Kuwata, K.; Haas, B. M.; Cao, Y. B.; Johnson, M. S.; Okumura, M. *J. Chem. Phys.* **1994**, *100*, 7153. (e) Dessent, C. E. H.; Bailey, C. G.; Johnson, M. A. *J. Chem. Phys.* **1995**, *103*, 2006.
- (a) Haines, S. R.; Geppert, W. D.; Chapman, D. M.; Watkins, M. J.; Dessent, C. E. H.; Cockett, M. C. R.; Müller-Dethlefs, K. *J. Chem. Phys.* **1998**, *109*, 9244.
- Chapman, D. M.; Müller-Dethlefs, K.; Peel, J. B. *J. Chem. Phys.* **1999**, *111*, 1955.
- Fujii A.; Miyazaki, M.; Ebata, T.; Mikami, N. *J. Chem. Phys.* **1999**, *110*, 11125.
- Geppert, W. D.; Dessent, C. E. H.; Ullrich, S.; Müller-Dethlefs, K. *J. Phys. Chem. A* **1999**, *103*, 7186.
- Puebla, C.; Ha, T. K. *THEOCHEM* **1990**, *64*, 203.
- Melandri, S.; Maccaferri, G.; Caminati, W.; Favero, P. G. *Chem. Phys. Lett.* **1996**, *256*, 513.
- Haines, S. R.; Dessent, C. E. H.; Müller-Dethlefs, K. *J. Chem. Phys.* **1999**, *111*, 1947.
- (a) Lipert, R. J.; Colson, S. D. *Chem. Phys. Lett.* **1989**, *161*, 303. (b) Fernandez, J. A.; Yao, J.; Bernstein, E. R. *J. Chem. Phys.* **1999**, *110*, 5159. (c) Le Barbu, K.; Brenner, V.; Millie, Ph.; Lahmani, F.; Zehnacker-Rentien, A. *J. Phys. Chem. A* **1998**, *102*, 128. (d) Hamabe, H.; Fukuchi, T.; Shiraishi, S.; Nishi, K.; Sekiya, H. *J. Phys. Chem. A* **1998**, *102*, 3880. (e) Hockridge, M. R.; Knight, S. M.; Robertson, E. G.; Simons, J. P.; McCombie, J.; Walker, M. *Phys. Chem. Chem. Phys.* **1999**, *1*, 407.
- Gerstenkorn, S.; Luc, P. *Atlas du spectra d'absorption de la molecule d'iode*; Laboratoire Aimé-Cotton CNRSII 91405: Orsay, France, 1978.
- Chupka, W. A. *J. Chem. Phys.* **1993**, *98*, 4520.
- Gaussian 94*, Revision E.1, Frisch, M. J.; Trucks, G. W.; Schlegel, H. B.; Gill, P. M. W.; Johnson, B. G.; Robb, M. A.; Cheeseman, J. R.; Keith, T.; Petersson, G. A.; Montgomery, J. A.; Raghavachari, K.; Al-Laham, M. A.; Zakrzewski, V. G.; Ortiz, J. V.; Foresman, J. B.; Cioslowski, J.; Stefanov, B. B.; Nanayakkara, A.; Challacombe, M.; Peng, C. Y.; Ayala, P. Y.; Chen, W.; Wong, M. W.; Andres, J. L.; Replogle, E. S.; Gomperts, R.; Martin, R. L.; Fox, D. L.; Binkley, J. S.; Defrees, D. J.; Baker, J.; Stewart, J. P.; Head-Gordon, M.; Gonzalez, C.; Pople, J. A. Gaussian, Inc.: Pittsburgh, PA, 1995.
- Calculations were also conducted at the B3LYP/6-31G* level of theory, but since the geometric structures, relative energies, and intermolecular frequencies were similar to those obtained using MP2/6-31G*, the results are not reported here.
- Gerhards, M.; Perl, W.; Kleinerhmanns, K. *Chem. Phys. Lett.* **1995**, *240*, 506.
- Calculations at the MP2/6-31G* level gave total energies of -494.549364, -494.549456, and -494.548886 hartrees for the S₀ states of the "oxygen in" analogues of isomers Ia, Ib, and II, respectively, versus -494.551823, -494.551904, and -494.551305 hartrees for the "carbon in" analogues.
- Gerhards, M.; Schiwek, M.; Unterberg C.; Kleinerhmanns, K. *Chem. Phys. Lett.* **1998**, *297*, 515.
- Bieske, E. J.; Rainbird, M.; Knight, A. E. W. *J. Chem. Phys.* **1991**, *94*, 7019.
- Takahashi, M.; Ozeki, H.; Kimura, K. *J. Chem. Phys.* **1992**, *95*, 6399.
- Peterson, K.; Dunning, T. H. *THEOCHEM* **1997**, *400*, 93.
- (a) Sadlej, J.; Buch, V.; *J. Chem. Phys.* **1994**, *100*, 4272. (b) Lundell, J.; Latajka, Z. *J. Phys. Chem. A* **1997**, *101*, 5004. (c) Yaron, D.; Peterson, K. I.; Zolandz, D.; Klemperer, W.; Lovas, F. J.; Suenram, R. D. *J. Chem. Phys.* **1990**, *92*, 7095.